ISTANBUL TECHNICAL UNIVERSITY ★ GRADUATE SCHOOL

MODEL BASED STATE OF CHARGE ESTIMATION OF ZINC-AIR BATTERIES

M.Sc. THESIS

Burak SATILMIŞOĞLU

Department of Control and Automation Engineering

Control and Automation Engineering Programme

DECEMBER 2021

ISTANBUL TECHNICAL UNIVERSITY ★ GRADUATE SCHOOL

MODEL BASED STATE OF CHARGE ESTIMATION OF ZINC-AIR BATTERIES

M.Sc. THESIS

Burak SATILMIŞOĞLU
(504171104)

Department of Control and Automation Engineering

Control and Automation Engineering Programme

Thesis Advisor: Prof. Dr. Fikret ÇALIŞKAN

DECEMBER 2021

İSTANBUL TEKNİK ÜNİVERSİTESİ ★ LİSANSÜSTÜ EĞİTİM ENSTİTÜSÜ

ÇİNKO-HAVA TİPİ BATARYALARDA MODEL TABANLI ŞARJ DURUMU KESTİRİMİ

YüKSEK LİSANS TEZİ

Burak SATILMIŞOĞLU
(504171104)

Kontrol ve Otomasyon Mühendisliği Anabilim Dalı

Kontrol ve Otomasyon Mühendisliği Programı

Tez Danışmanı: Prof. Dr. Fikret ÇALIŞKAN

ARALIK 2021

Burak SATILMIŞOĞLU, a M.Sc. student of ITU Graduate School student ID 504171104, successfully defended the thesis entitled "MODEL BASED STATE OF CHARGE ESTIMATION OF ZINC-AIR BATTERIES ", which he/she prepared after fulfilling the requirements specified in the associated legislations, before the jury whose signatures are below.

Thesis Advisor :	**Prof. Dr. Fikret ÇALIŞKAN** Istanbul Technical University	.....
Jury Members :	**Prof. Dr. Şeref Naci Engin** Yildiz Technical University	.....
	Doç. Dr. Osman Kaan Erol Istanbul Technical University	.....

Date of Submission : 15 November 2021
Date of Defense : 10 December 2021

To my family,

FOREWORD

I would like to thank Prof. Dr. Fikret Caliskan for excellent guidance and support during this process. Also I want to present my gratitutes to the Prof. Dr. Ibrahim Eksin for continous help to me starting from master education. I also appreciate to my family and friends who kept me motivated. I would also like to thank FEV Turkey family & Dr. Murat Demirci for providing me a great ambiance during my master education.

December 2021 Burak SATILMIŞOĞLU

TABLE OF CONTENTS

Page

ABBREVIATIONS

Ah	**:** Ampere Hour
BMS	**:** Battery Management System
DOD	**:** Depth of Discharge
ECM	**:** Equivalent Circuit Model
EV	**:** Electric Vehicle
HV	**:** High Voltage
HPPC	**:** Hybrid Pulse Power Characterization Test Procedure
I	**:** Current(A)
LTI	**:** Linear Time Invariant
Li-Ion	**:** Lithium Ion
NEDC	**:** New European Driving Cycle Test Procedure
OCV	**:** Open Circuit Voltage
P	**:** Electrical Power
SoC	**:** State of Charge
SoH	**:** State of Health
T	**:** Temperature in Kelvin(K)
U	**:** Voltage
Wh	**:** Electrical Energy
WLTP	**:** Worldwide Harmonised Light Vehicles Test

LIST OF TABLES

Page

LIST OF FIGURES

Page

MODEL BASED STATE OF CHARGE ESTIMATION OF ZINC-AIR BATTERIES

SUMMARY

Electric vehicles have increased their popularity in the last 30 years. They provide more environmentally friendly and sustainable transportation than internal combustion engine vehicles and have led the transportation industry to research this area.

Today, batteries in lithium-ion chemistry are widely used in electric vehicles. However, although it is widely used, researchers have led researchers to research different battery chemistries due to the raw material problems encountered in the production processes, the inability to reach the desired range, long charging times, and high costs.

As a result of these researches, batteries in metal-air chemistry have started to gain importance recently. It is foreseen that it will be used widely in the future due to its energy density advantage against lithium-ion chemistry, its much shorter charging times, and its environmentally friendly nature.

Since it is known that a single cell of this battery chemistry, which is expected to be used in the future, cannot meet the energy needs of electric vehicles due to theoretical limits, multiple cells will be connected in series and parallel to form a battery pack. Controlling this structure formed by bringing together many cells through a battery management system is a natural requirement due to safety, efficiency, and performance criteria. Battery management systems, which control each cell's charge and health status, ensure that the system operates safely and in ideal conditions.

Battery management systems measure the values of the cells such as voltage, current, temperature, and control the batteries over observable parameters and monitor the battery charge status, which cannot be measured directly by making a model-based estimation. The accuracy of these estimations is crucial because it allows the battery to be used within safe limits and is directly related to the range of electric vehicles.

In this study, a LPV cell model created for the zinc-air type batteries, which are thought to be used frequently in the future because of their high specific energy, cost-effectiveness, and environmental friendliness by using experimental data. Then, proposed model is validated against validation data.

After reaching the desired cell simulation model, the battery state of charge is obtained by using two different methods, the ampere-hour counting method, and the extended Kalman filter method. Ampere hour counter method is a reliable model in the simulation environment since there is no disturbance is present. The Extended Kalman filter method is good at estimating state of charge in the noisy, real-world environment. By comparing the ampere-hour counting method, and the extended Kalman filter

method, the confidence of the estimation is gained. Then, the performance of extended Kalman filter method is tested against noisy measurement data.

ÇİNKO-HAVA TİPİ BATARYALARDA MODEL TABANLI ŞARJ DURUMU KESTİRİMİ

ÖZET

Elektrikli araçlar, içten yanmalı motorlu araçlara göre daha çevreci ve sürdürülebilir bir ulaşım sağlaması nedeniyle geçtiğimiz 30 yılda popülerliğini arttırmış ve ulaşım endüstrisini bu alanda araştırmalar yapmaya yöneltmiştir.

Günümüzde, elektrikli araçlarda yaygın olarak lityum iyon kimyasındaki bataryalar kullanılmaktadır. Yaygın şekilde kullanılıyor olmasına karşın üretim süreçlerinde karşılaşılan hammadde problemleri başta olmak üzere, kullanıcıların istediği menzile ulaşılamaması, uzun şarj süreleri ve yüksek maliyetler nedeniyle araştırmacıları farklı batarya kimyalarını araştırmaya yöneltmiştir.

Yapılan bu araştırmalar sonucunda metal-hava kimyasındaki bataryalar son zamanlarda önem kazanmaya başlamıştır. Lityum-iyon kimyasına karşı sahip olduğu enerji yoğunluğu avantajı başta olmak üzere, çok daha kısa şarj sürelerine sahip olması ve görece çevreci olması nedeniyle ileride yaygın olarak kullanılmaya başlanılacağı öngörülmektedir.

Lityum-iyon batarya tipinin teorik olarak sahip olduğu enerji yoğunluğunun bir dizel yakıta oldukça yakın olduğu bilindiğinden, araştırmacılar nihai hedeflerini bu batarya kimyasının kullanılması olarak belirlemişlerdir, ancak var olan hammadde sıkıntısı ve lityum kaynaklarına olan erişimin limitli olması nedeniyle çeşitli metaller de araştırmacıların radarına girmiştir. Yapılan bu araştırmaların sonucunda, lityumun yeni nesil bataryalar için tek kaynak olmadığı, çeşitli metallerin de lityum-iyon batarya kimyasından daha iyi karakteristikler vaadettiği görülmüştür. Bu sebeple, özellikle lityum-hava tipi bataryalara geçiş sürecinde kullanılmasının beklenildiği, ülkemizde de hammaddesi bulunan, çinko-hava tipi bataryalar üzerinde bir çalışma yapılmıştır.

İleride çokça kullanılacağı öngörülen bu batarya kimyasının, tek bir hücresinin elektrikli araçların enerji ihtiyacını karşılayamacağı teorik limitlerden dolayı bilindiğiden, birden çok hücre birbirlerine seri ve paralel bağlanarak bir batarya paketi oluşturularak kullanılacaktır. Pek çok hücreyi bir araya getirerek oluşturulan bu yapının bir batarya yönetim sistemi vasıtasıyla kontrol edilmesi, güvenlik, verimlilik ve performans kriterlerinden ötürü doğal bir gerekliliktir. Her bir hücrenin şarj ve sağlık durumunu kontrol eden batarya yönetim sistemleri, sistemin güvenli ve ideal koşullarda çalışmasını sağlamaktadır.

Batarya yönetim sistemleri, hücrelere ilişkin gerilim, akım, sıcaklık gibi değerleri ölçerek, gözlenebilir parametreler üzerinden bataryaları kontrol etmekle beraber, doğrudan ölçülemeyen batarya şarj durumunu model tabanlı kestirim yapmak suretiyle gözlemektedir. Yapılan bu kestirimlerin doğruluğu, bataryanın güvenli sınırlar içerisinde kullanılmasını sağlamasından ötürü ve elektrikli araçların menziliyle doğrudan ilişkili olduğu için önem arz etmektedir.

İkinci bölümde, literatürde bulunan, günümüzde sıkça kullanılan batarya kimyaları incelenmiş, metal-hava batarya kimyası ve tercih edilen batarya tipinden ayrıca bahsedilmiştir.

Sonrasında, şarj tahminlemede kullanmak üzere hücrenin dinamik davranışını modellemenin gerekli olduğu bilindiğinden, hücre modellemesi üzerinde çalışma yapılmıştır. Eşdeğer devre modeli başta olmak üzere çeşitli modeller tanıtılmış, sonrasında ise parametreleri bataryadan çekilen akıma bağlı değişken bir model yapısı kurgulanmıştır. Kurgulanan bu modelin parametrelerinin belirlenmesi için deney verilerinden yararlanılmış olup, çeşitli çalışma noktaları belirlenmiştir. MATLAB parameter estimation toolbox yardımıyla belirlenen çeşitli çalışma noktaları için doğrusal modeller elde edilmiştir.

Elde edilen bu modellerin yalnızca belirlenen çalışma noktası etrafında bataryanın dinamik davranışını başarıyla modellediği, çalışma noktasından uzaklaştıkça model davranışının batarya davranışından farklı olduğu görülmüştür. Batarya davranışının deşarj akımıyla değiştiği bilindiğinden, model parametrelerinin deşarj akımına bağlı olarak değiştirilmesi planlanmış ve her bir model parametresine birinci ve ikinci dereceden polinomlar uydurulmuştur. Elde edilen nonlineer batarya modeli, eğitim veri setinden farklı veriler kullanılarak doğrulanmış ve batarya davranışını, çeşitli akımlar çekilmesine rağmen başarıyla temsil ettiği görülmüştür.

Dördüncü bölümde ise endüstride sıkça kullanılan yöntemlerden biri olan akım sayma yöntemi ele alınmış olup, bu yöntem kullanılarak, açık devre gerilimi ve bataryada bulunan akım sensörü verileri kullanılarak batarya şarj durumu tahminlemesi yapılmıştır. Simulasyon ortamında çok yüksek doğrulukla çalışan bu model, daha sonrasında genişletilmiş kalman filtresinin validasyonunda kullanılmıştır. Gürültülere karşı hassaslığı ve gerçek hayatta karşılaşılabilecek zorlukları minimuma indirmek amaçlı bir filtre yapısının kullanılmasına ihtiyaç duyulduğu tespit edilmiş olup, buna çözüm olarak genişletilmiş kalman filtre yapısı incelenmiştir.

Model tabanlı bu filtre yapısının uygulanabilmesi için öncelikle sisteme ilişkin durum-uzay denklemleri çıkarılmış olup, taylor serisi açılımı yardımıyla kalman denklemleri elde edilmiştir. Elde edilen bu denklemler MATLAB/Simulink ortamında gerçeklenmiş olup, deney verileri ve akım sayma yöntemi kullanılarak doğrulanmıştır.

Sonuç olarak, elde edilen veriler gerçek sonuçlarla karşılaştırılmış olup, batarya kimyasının stabil olmamasından kaynaklanan ve laboratuvar tipi bir batarya setinin verilerinin kullanılmasına rağmen batarya şarj durumu kestirimi başarılı bir şekilde yapılmıştır.

Son bölümde ise yapılan çalışmaya ilişkin bilgiler verilmiş olup, çalışmanın limitleri anlatılmış ve gelecekteki araştırmacılara yönelik olarak çeşitli iyileştirme seçenekleri belirtilmiştir.

1. INTRODUCTION

In recent years, electric vehicles have become a phenomenon of society transformations towards a sustainable future. Vehicle manufacturers and policymakers are increasing their attention and action on electric vehicles (EVs). This is because EV technologies are attractive options to achieve environmental, societal, and health goals.

EVs are not only two to four times more efficient than conventional internal combustion engine models, but they can also reduce dependence on petroleum-based fuels and, when powered by low-carbon electricity, lead to significant reductions in greenhouse gas emissions. In addition, because EVs produce no tailpipe emissions, they are well suited to solving air pollution problems. In addition, EVs are driving advances in battery technology, a key issue for industrial competitiveness in the transition to clean energy. [13]

Today, battery technology is the bottleneck of electric vehicles. In order to overcome that problem, the academy and industry are widely researching on that topic. Even though lithium-ion batteries are widely used today, the other battery chemistries are promising in order to reach a longer range and environment-friendly goals.

1.1 Purpose of Thesis

The purpose of this thesis is to investigate one of the promising battery chemistry, zinc-air batteries. Due to properties such as high energy and high power density and the environment-friendly production possibilities, zinc-air batteries are gaining attention from society.

However, the advantages of the batteries come with safety concerns. Batteries could be sensitive to overcharging, undercharging, short circuits, and temperature deviations. [14] [15] In order to operate the batteries in secure and optimal conditions, the Battery Management Systems(BMS) are used to monitor battery cells.

BMS could monitor battery temperatures, voltages, and currents but the state of charge cannot be measured directly. A robust and precise model needs to be employed to ensure safe and secure battery operation.

In this work, a robust model for zinc-air is obtained. From that model, state of charge estimation with Extended Kalman filters are employed and results are compared.

2. LITERATURE REVIEW

2.1 Terminology

Battery and hybrid electric vehicle terminology are defined at SAE J1715. [16] In this section, a few of the common ones will be introduced.

2.2 Battery Technologies

Table 2.1 : Comparison of the Different Batteries.

Battery Chemistry	Voltage(V)	Specific Energy Density (Wh/kg)
Lead Acid	2.1	30-50
NiCd	1.2	50-75
NiMh	1.2	70-95
LiFePO4	3.2	120
NMC	3.6	118-250
Zinc-Air	1.65	1085

2.2.1 Lead acid batteries

French physician Gaston Plante invented in 1859. Lead-acid batteries comprise of flat lead plates immersed in a pool of electrolytes. This pool of electrolytes consists of water and sulfuric acid. As the battery discharges the electrolyte coats the lead plates and this process is called lead sulfate(sulfation). Lead sulfate is a soft material and can be reconverted back into the lead and sulfuric acid. But to reconvert it the battery should be recharged immediately. If the battery is not promptly recharged, the lead sulfate will begin to form hard crystals and will be unable to be converted back to regular voltage levels. Most of the LA batteries are formed by two 6 volt batteries or a single 12 volt battery. Both of these varieties are constructed from several cells connected next to each other while each cell produces approximately 2.1 volts. LA is used as a 12V power supply system of vehicles, uninterruptible power supplies, and several back-up power supplies. Energy density values are different based on the

technology but they are between 30 to 50 Wh/kg with up to 1500 cycle life and cell voltages are around 2V [17].

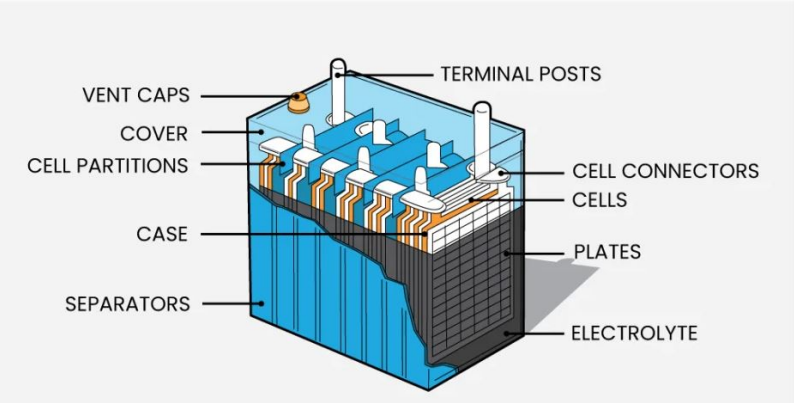

Figure 2.1 : Lead Acid Battery Structure [3].

2.2.2 Nickel based batteries

2.2.2.1 Nickel-cadmium batteries

Nickel-based batteries invented by Waldemar Jungner in 1899. It has several advantages over the lead-acid type of battery. Because of the high discharge rates, capacity advantages, and stability advantages over the lead-acid battery, it was the preferred battery choice for the airline industry, medical industry for many years.

The Nickel Cadmium type batteries have nickel species as positive electrodes and cadmium or electrodes species as negative electrodes and alkali solution KOH as the electrolyte.

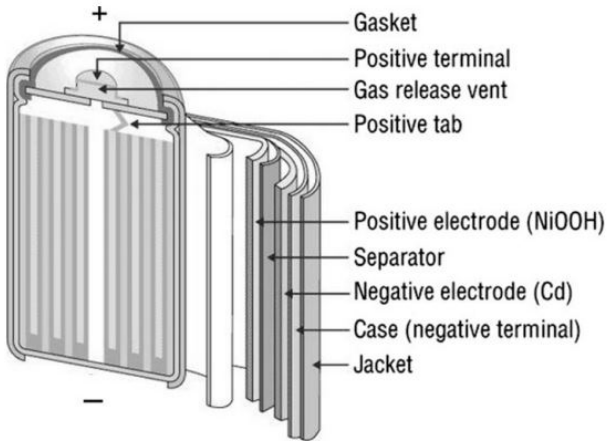

Figure 2.2 : Nickel-Cadmium Battery Structure [4].

Most of the nickel-based batteries have 1.2V nominal cell voltages. Usually, it consists of 10 series of battery cells to use as a 12V power supply. They are mostly preferred for client electronics because of their resilience and low maintenance needs. Energy density values are between 50-75 Wh/Kg with over 3500 cycle life.

Even though NiCd type of battery offers good technical specifications, it has major drawbacks such as considerable costs over lead-acid batteries ($>$ 10 times) and toxicity of the battery materials [4].

2.2.2.2 Nickel-metal hydride batteries

That battery chemistry is similar to the Nickel Cadmium type of batteries. The main difference comes from the electrolyte, by eliminating the cadmium from the battery, toxicity level decreases during battery capacity increases.

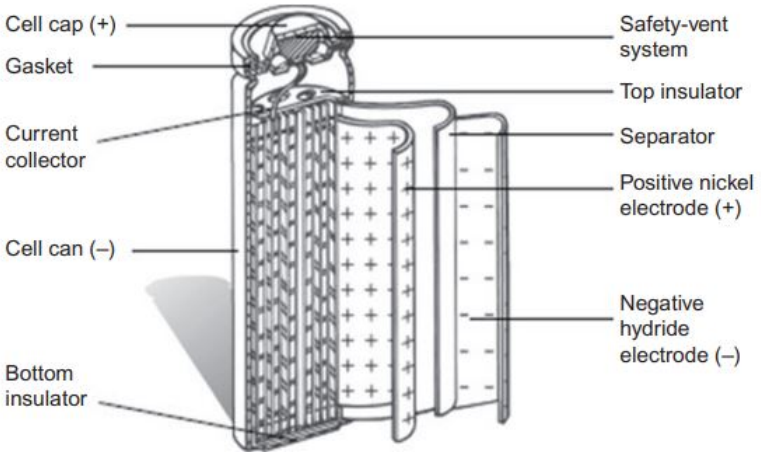

Figure 2.3 : Nickel-Metal Hydride Battery Structure [5].

With the metal electrolyte, Nickel-Metal Hydride chemistry offers 70-100 Wh/Kg energy density with around 1000 cycle life. Because of the high volumetric energy (170-420 Wh/L) and discharge capabilities, that batteries are mostly employed in electric vehicles and various power sources in the industry [4].

Figure 2.4 : NiMH Battery utilized Toyota Prius [5].

2.2.3 Lithium based batteries

Lithium-ion batteries were first proposed in 1912 by G.N. Lewis. Even though extensive researches were conducted, the first commercial rechargeable battery produced in 1991 by Sony. Lithium-ion batteries have superior cycle life, power density, and low power loss capabilities.

The cells are made from anode cathode plates, filled with liquid electrolytes, and plates are separated by a separator. Usually, the cathode is a metal oxide, and the anode material is graphite.

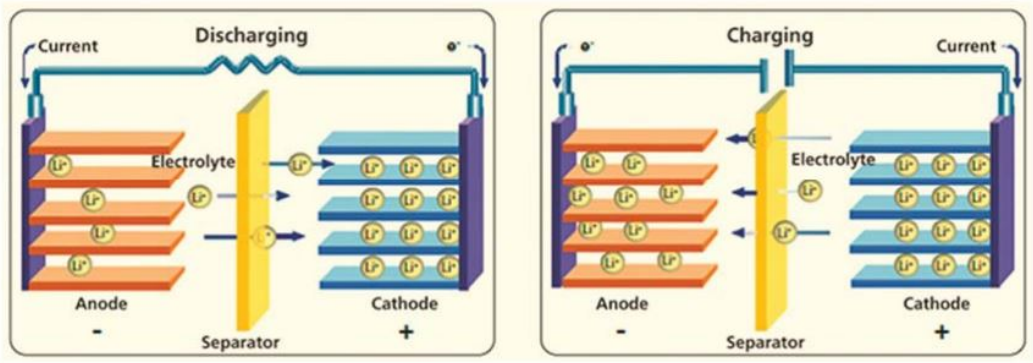

Figure 2.5 : Basic Working Principle of Lithium Ion Batteries [6].

As shown in Figure 2.5, during discharging lithium ions goes from anode to cathode through the electrolyte, while charging it works other way around.

Because of the promising technical capabilities, that chemistry is extensively researched from both academia and industry and has been used for almost all applications. However, lithium-ion batteries have major safety issues. Due to the nature of the lithium, handling of that batteries is critical because metal oxides are thermally unstable, and poor handling could lead to the thermal runaway. To minimize that risk, lithium-ion batteries usually comes with a separate battery management system to monitor system states, avoiding over-voltage, under-voltage errors, and safely handling of the lithium-ion batteries.

Each application and industry has its own special requirements. Those could be the specific energy, specific volume, eco-friendliness, cycle life, etc,. to meet each requirement, different cathode structures are also employed.

2.2.3.1 Lithium iron phosphate($LiFePO_4$)

Lithium-ion phosphate(LFP) type batteries invented in 1996 by Texas University researchers. It was commercially available in 1999, considering the longer lifespan, low maintenance requirements, and high specific power than other types of batteries it gained a lot of attention at that time.

Due to the low specific energy, packaging of the batteries for electric vehicles is problematic, hence LFP was mainly used by electric trucks and caravans because of the packaging volume. It has 90-120 Wh/kg specific energy with more than 2000 cycle life.

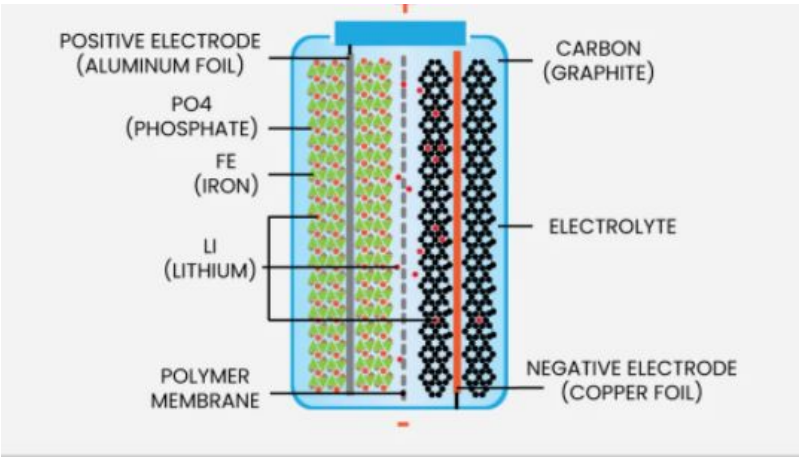

Figure 2.6 : Lithium Iron Phosphate Battery [7].

2.2.3.2 Lithium nickel cobalt manganese oxide(NMC)

The lithium nickel cobalt manganese oxide(NMC) batteries were introduced in the early 1980s but their first commercial appearance was in 1995. The main advantage of that chemistry is combining nickel and manganese specifications in one battery. Nickel is known for its high specific energy capacity, while manganese has low internal resistance [18]. Thus, combining both metals enhanced each other's capabilities and NMC chemistry became the most successful lithium-ion battery chemistry.

Even today, NMC chemistry is leading the battery market. Almost all of the available electric vehicles are using that chemistry because of its advantages.

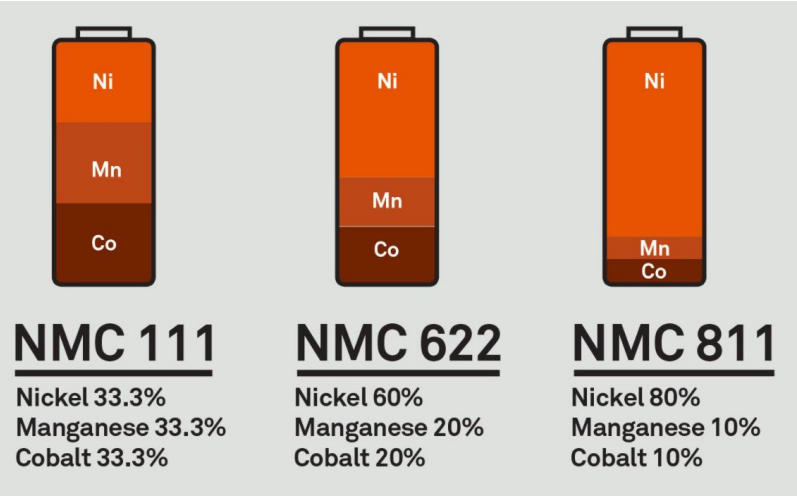

Figure 2.7 : Different NMC Battery Variations.

Industry leaders are widely researching and have been improving new NMC combinations to compete against next generation battery technologies, improve energy efficiency, and reduce costs.

2.2.4 Metal-air batteries

Even though lithium-ion battery technologies have been widely researched, industry and academia still improving the battery technologies. Safety issues, high energy needs, raw material problems, and price leads to the research of metal-air batteries.

In comparison to lithium batteries, the density of energy and price advantages are significantly better for metal-air batteries.

The way of working is different from other kinds of batteries. Metallic ions are transformed from the anode to the cathode in classic ionic batteries. Metals or alloys change into metallic ions at the anode of metal-air batteries, while oxygen transforms into hydroxide ions at the cathode. [8].

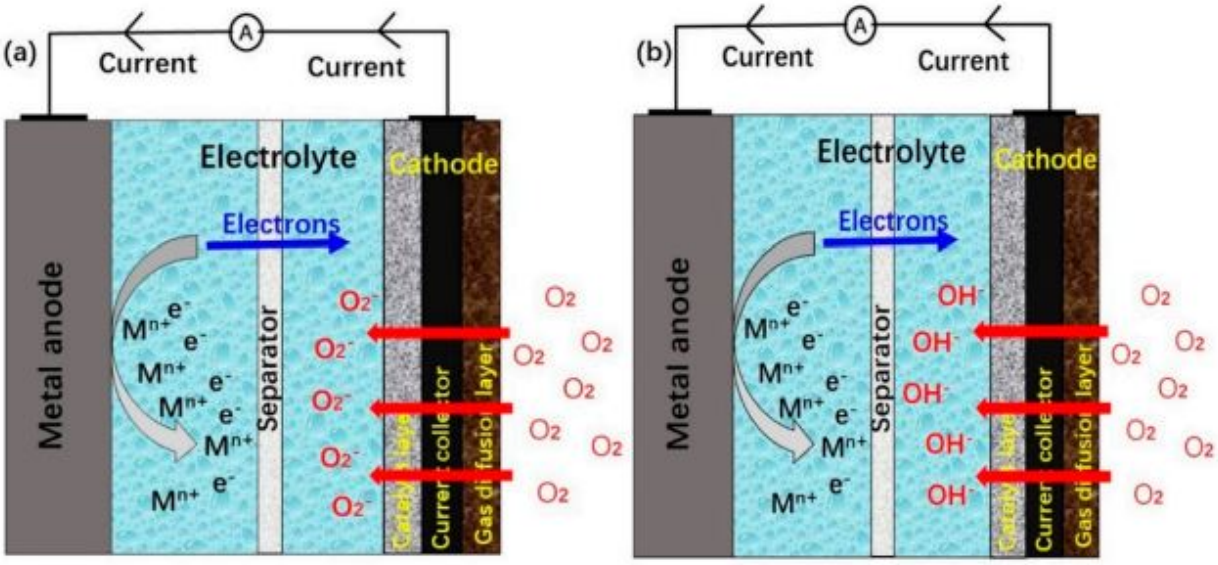

Figure 2.8 : Schematic Diagram of MAB Battery Variations [8].

Different packaging, different cathode variations are still in the development phase, road blockers are mainly safety and aging-related issues.

Table 2.2 : Comparison of the Different Metal Air Batteries [1].

Battery Chemistry	Voltage(V)	Theoretical Specific Capacity (Ah/Kg)	Theoretical Energy Density (Wh/Kg)
K-Air	2.48	377	935
Na-Air	2.27	487	1105
Al-Air	2.7	1030	2791
Mg-Air	3.09	920	2843
Zinc-Air	1.65	658	1085
Li-Air	2.96	1170	3463

As shown in Table 2.2, even though lithium-air battery chemistry has shown superior theoretical capabilities. In reality, it is far from commercial use because of the safety, rechargeability, and cost issues. In that sense, reliable, safe, and cheap cathode materials are gaining attention from researchers.

2.2.4.1 Zinc-air batteries

Zinc-air batteries have attracted interest over recent years as a possible commerciable alternative of lithium-ion technology. Zinc-air batteries are promising because of the environmental friendliness, theoretical energy density(1085 Wh/Kg), considerably low cost(<10$ potentially), and inherent safety. [19]

Primary zinc-air batteries have been employed effectively in the fields of the hearing aid industry, GPS systems, and railway signal equipments. Rechargeable zinc-air batteries have just recently evolved and have seen tremendous growth. Furthermore, by physically swapping the battery electrode and liquids, this sort of battery may be manually refilled. Because mechanical recharging has no significant challenges, it is possible to have quick refueling capabilities similar to petrol refill. [10].

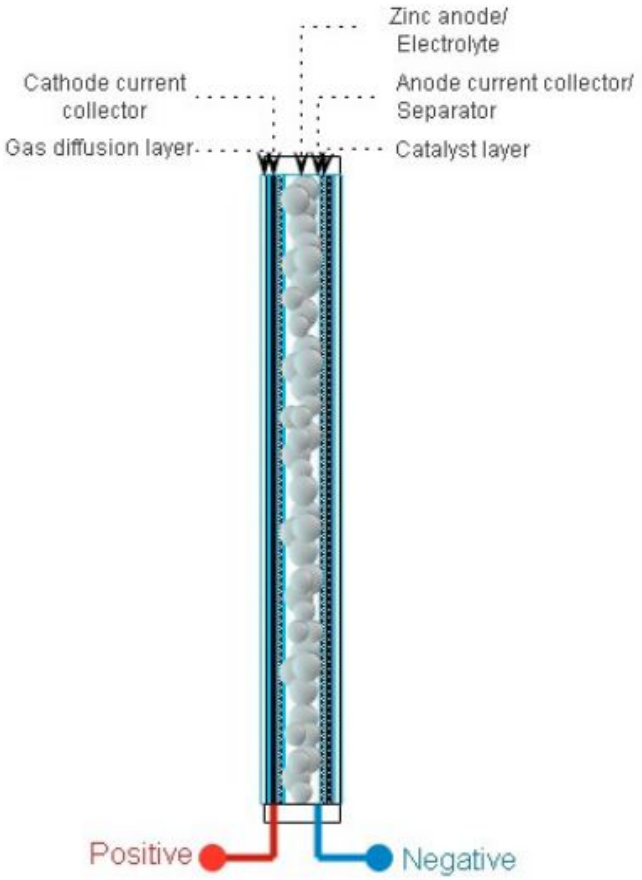

Figure 2.9 : Structure of zinc-air battery cell [9].

Researchers from all around the globe have lately addressed these zinc battery topologies with the goal of overcoming long-standing drawbacks like as low cyclability by inventing novel electrode materials, formulations, and battery designs. This newfound interest in zinc-based battery technology is gathering researchers from several sorts of backgrounds, bringing interesting new insights to the quest. [20]

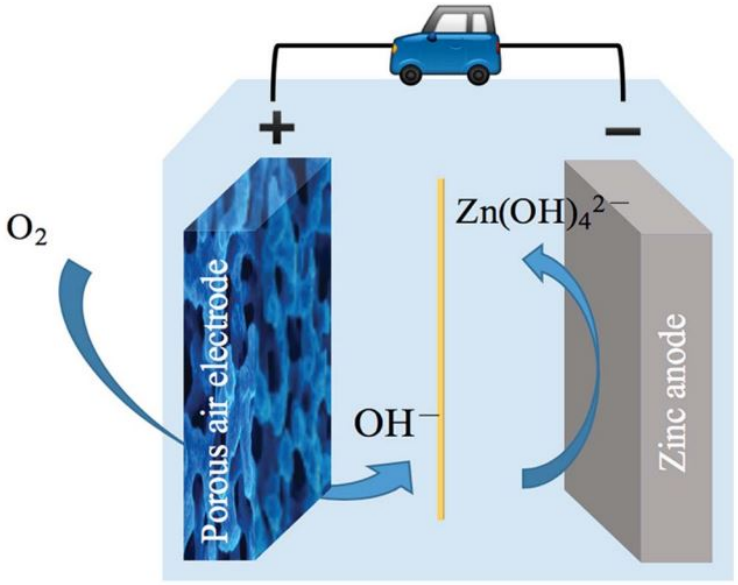

Figure 2.10 : Schematic of zinc-air battery cell [10].

The basic working principle of these batteries is, during discharge the zinc anode gets oxidizes and interacts with OH^- to produce soluble zincate ions. When these zincate ions get supersaturated in the electrolyte, they decompose spontaneously to generate an insoluble zinc oxide. [10]

Due to the inherent safety characteristics and high volumetric energy density, zinc-air batteries can be employed to work in the electric vehicle industry. In this work, cell from this chemistry is going to be employed.

3. CELL MODELLING AND PARAMETER IDENTIFICATION

In this chapter, a model that represents the battery will be developed. The model will be developed by using the discharge data of the zinc-air battery. First, We will start to employ the 1st order RC model, and then the parameter varying model will be employed to represent the high non-linearity of the model. This chapter introduces the most common models and describes the employed model for this thesis.

3.1 Utilized Battery Cell

As discussed in the previous chapter, zinc-air chemistry is capable of take-over the market in upcoming years. Because of that, in this thesis, a zinc-air type battery is going to be used. Characteristics and cell structure is given below.

Table 3.1 : Summary of cell parameters [2].

Parameters	Values
KOH Concentration	8 M
Seperator Thickness	0.1mm
Cathode Thickness	1 mm
Cathode Length	9.5 cm
Cathode Active Surface Area	29.83 cm^2
Catalyst Loading	3 $mgcm^{-2}$
Amount of Zinc	6 g
Electrolyte Volume	15 cm^3
Anode Current Collector Diameter	5mm
Anode Current Collector Full Length	20.5 cm
Zinc Pellets Bed Length	13.5 cm
Anode chamber diameter	10 mm

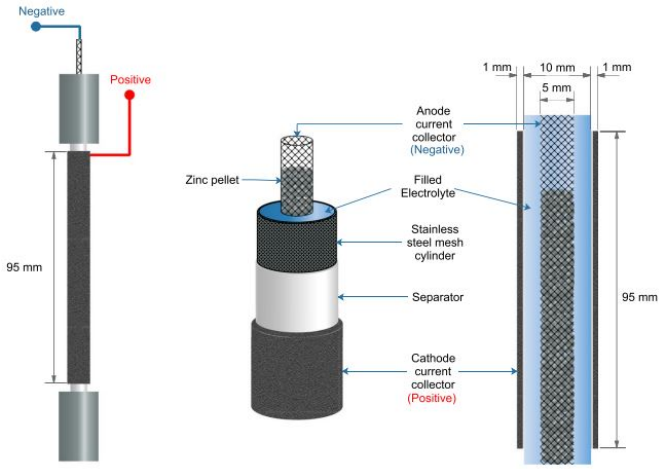

Figure 3.1 : Utilized battery cell.

3.2 Equivalent Circuit Model

Batteries are known for complex and highly nonlinear behaviours. Although the non-linearity & complex electrochemical chemistry that batteries have, basic electrical components can be used to represent the dynamic behaviour of the batteries.

Battery equivalent circuit models are widely employed in industry and academia to represent the complex electrochemical behaviour of batteries. [21] There are many equivalent circuit models are available to represent battery behaviour, some of them are using passive elements while other structures are using active components or adaptive functions.

The fundamental model uses only voltage source as a function of the state of charge but to increase accuracy different model structures can be obtained.

3.2.1 Basic model

The basic model is built by only internal resistance and voltage source dependent on the state of charge of the battery. The basic model can only represent the voltage drop of the battery -if current occurs-.

As shown in Figure 3.2, implementation is simple, but accuracy is not enough to estimate the state of charge of the battery.

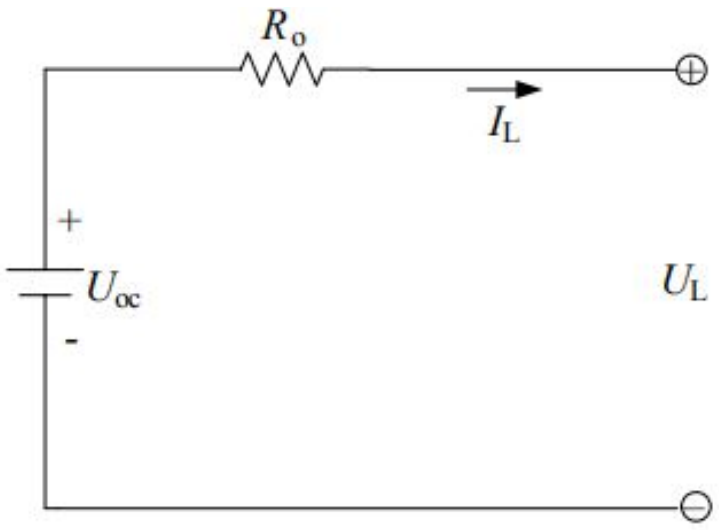

Figure 3.2 : Basic Battery Model.

$$U_L = U_{oc}(SoC) - I_L R_0 \tag{3.1}$$

To increase model accuracy, internal resistance can be employed dynamically with respect to the charging, discharging state, and state of charge of the battery.

3.2.2 R_{int} model

As illustrated in Figure 3.3, R_{int} model consists of the same elements as the basic model but the differences are, either battery open circuit voltage and resistance elements are functions of the state of charge, charge current, and discharge currents. [22]

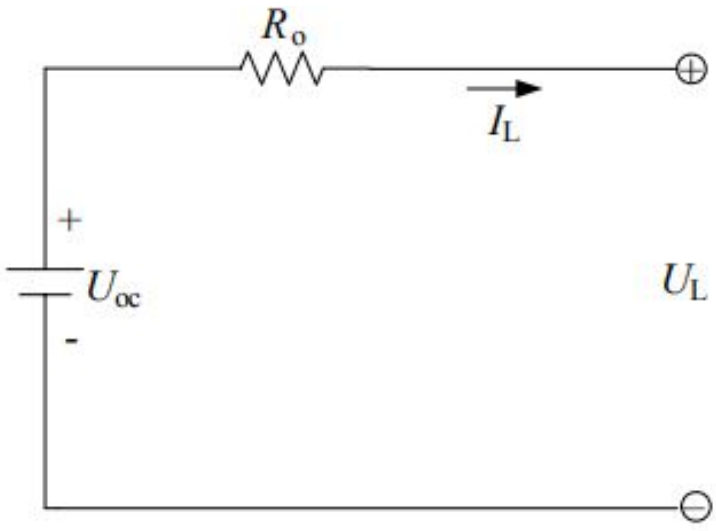

Figure 3.3 : R_{int} Battery Model.

$$U_L = U_{oc}(SoC) - I_L R_0(SoC) \quad \textbf{(3.2)}$$

Even though that model structure gives better performance than the basic model, transient dynamics of the battery can not be represented by using that model structure. Thevenin model structure could also capture the transient model dynamics.

3.2.3 Thevenin model

A typical thevenin based battery model structure consists of DC resistance R_0 and from one to multiple RC pairs to represent battery dynamics. The first order RC model shown in Figure 3.4.

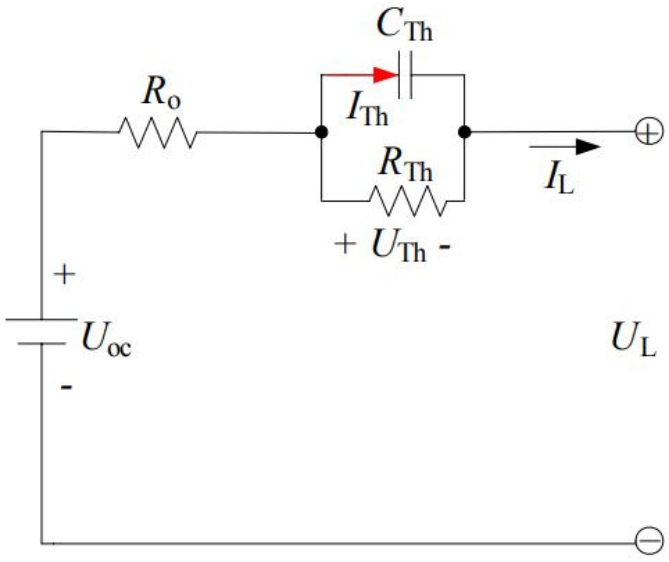

Figure 3.4 : First Order RC Model.

$$I_L = I_C + I_R \tag{3.3}$$

$$U_L = U_{oc}(SoC) - R_0 I_L - U_{th} \tag{3.4}$$

Internal resistance represented by R_0, RC branch is used to catch transient response of the battery mostly during current changes. To capture all dynamics of the battery, increasing the order of the model is possible.

But due to the computational effort, first and second order RC models are widely used in applications.

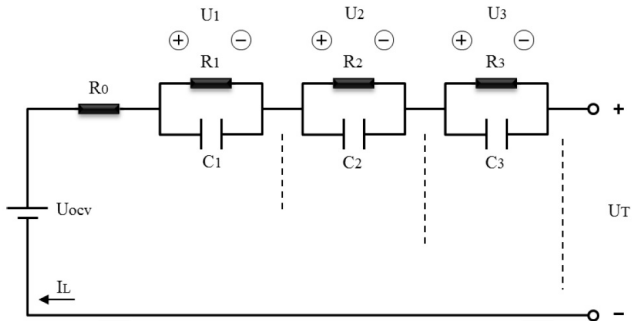

Figure 3.5 : Third Order RC Model.

3.3 Linear Parameter-Varying(LPV) Model

Linear parameter varying model type is a generic type of the LTI form, constructed based on the notion that dynamic attributes vary depending on the operating conditions. [11] The dynamic properties of the battery are current, temperature, and state of charge of the battery.

With respect to the experimental results from the test cell, the discharge current is selected as a scheduling parameter for the battery model. The general state space representation could be written with respect to the scheduling function p, as below;

$$x(k+1) = A(p(k)).X(k) + B(p(k)).u(k) \tag{3.5}$$

$$y(k) = C(p(k)).X(k) + D(p(k)).u(k) \tag{3.6}$$

3.4 Parameter Determination

The parameters of the battery cell will be determined by using experimental data. [2] To be able to model precisely, various scheduling spaces were selected then linear models were obtained & assigned to the respective points.

Given experimental data is only available from 100mA to 1000mA. Operating points were selected as 100mA, 450mA, and 900mA discharge currents.

State space representation of the linear model is given below;

$$x(k+1) = A.X(k) + B.u(k) \tag{3.7}$$

$$y(k) = C.X(k) + D.u(k) \tag{3.8}$$

where u is an input vector, y is output. Hence, input is current, the output is the potential loss of the battery, u is current, y is the potential loss of the battery cell.

Training experiment data are used to estimate model parameters by using the parameter estimation toolbox in MATLAB Simulink.

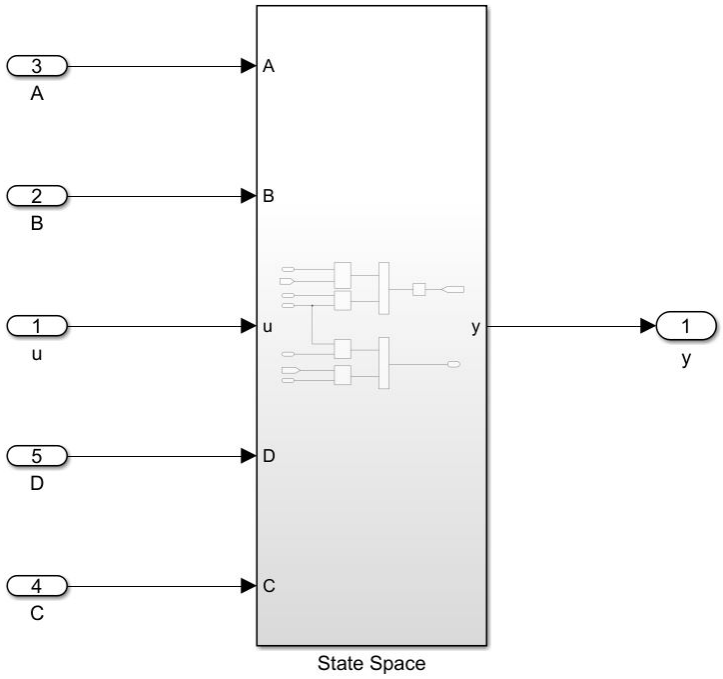

Figure 3.6 : State Space Model Implementation.

As shown in Figure 3.6 & Figure 3.7, the linear model implemented in Simulink. At the initial state, model parameters are selected from random variables, then test data is fed through the model, where input is current, the output of the model is selected as a potential loss across the battery.

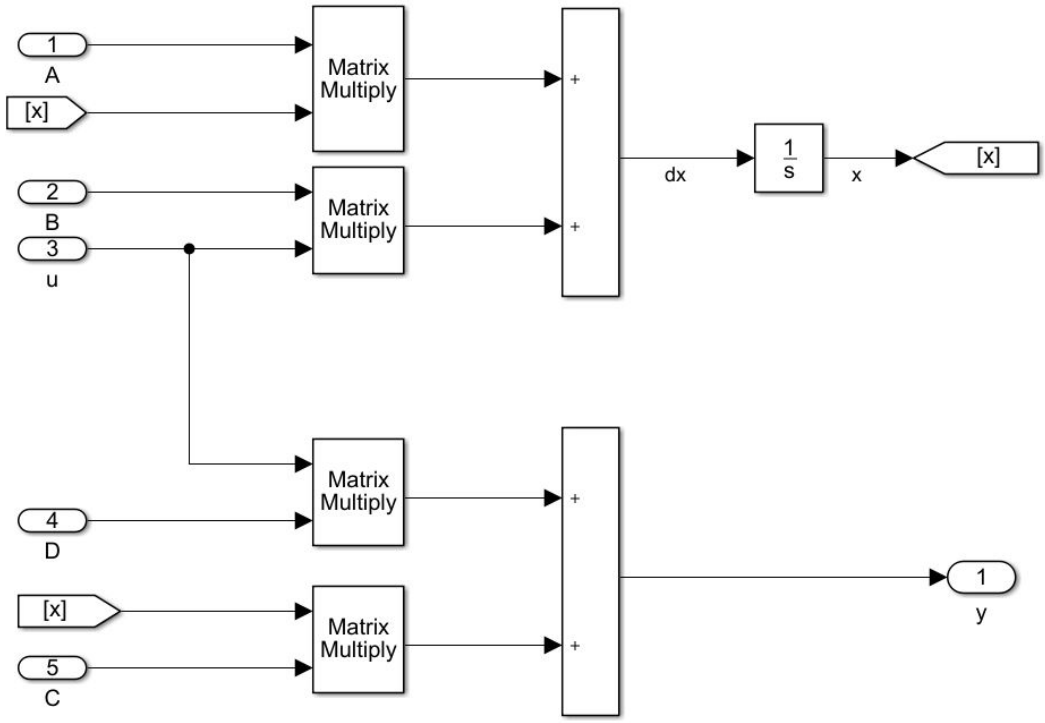

Figure 3.7 : State Space Model Implementation.

The test data for one of the selected operating point is shown in Figure 3.8.

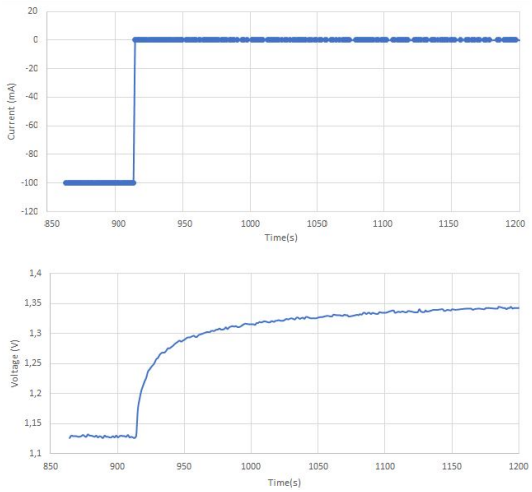

Figure 3.8 : Test Data for 100mA Operating Point [11].

After assignment and intensive optimization procedure, model parameters are estimated with less than % 2 sums of squared error.

Then that estimation procedure is applied for all selected operating points. For each operating point, three different models are obtained from different training data. In total, 18 different models were obtained for respective operating points.

Table 3.2 : Obtained Model Parameters.

Operating Point	A	B	C	D
100mA Discharge-1	0.8884	0.6472	0.3354	0.1289
100mA Discharge-2	0.8754	-0.5749	-0.3609	0.4943
100mA Discharge-3	0.8771	-0.5085	-0.4326	0.4338
100mA Charge-1	0.9503	-0.1232	-0.6526	0.4655
100mA Charge-2	0.9567	0.0972	0.7609	0.4657
100mA Charge-3	0.9583	0.0953	0.7491	0.5067
450mA Discharge-1	0.6433	-0.5054	0.3494	0.5297
450mA Discharge-2	0.7362	0.2783	0.5664	0.4718
450mA Discharge-3	0.7421	0.2123	0.8705	0.3711
450mA Charge-1	0.9132	-0.0506	-1.1848	0.3504
450mA Charge-2	0.9349	-0.0357	-1.2178	0.4012
450mA Charge-3	0.9421	-0.0313	-1.2382	0.4174
900mA Discharge-1	0.7885	-0.1840	-0.1394	0.6378
900mA Discharge-2	0.6926	0.1188	0.9818	0.3954
900mA Discharge-3	0.7572	0.0947	0.9454	0.4209
900mA Charge-1	0.9251	-0.0220	-1.2967	0.3702
900mA Charge-2	0.9426	-0.0166	-1.4480	0.3545
900mA Charge-3	0.9208	0.0258	1.4075	0.3191

Comparison of the results are showing that linear models are representing the battery potential loss behaviour with high precision around the operating point of the battery.

When models are used for a different condition than the operating condition, model behaviour is poorly estimating the actual response. Thus, the linear models could properly foresee the response behaviour, if the current level is arranged accordingly.

From that point, it could be understood that the linear model is only capable to imitate battery behaviour around the same operating point. Because the gain of the model is differentiating from each other. To obtain one model that is capable to work for each operating condition, all of the obtained linear models need to be combined. In this situation, LPV model parameters need to be found.

LPV model parameters are shown in Table 3.2 above. For each model parameter, a polynomial function needs to be assigned with respect to the LPV equations 3.7 and 3.8.

Parameter A and D were having consistent behaviour, second order polynomial could be fitted. However, parameters B and C were showed are inconsistent trend. To address that issue, C is fixed as unit gain, B and C multiplied together to have a consistent model parameter. [11]

After that assignment, the LPV model becomes;

$$x(k+1) = A(p(k)).X(k) + BC(p(k)).u(k) \tag{3.9}$$

$$y(k) = X(k) + D(p(k)).u(k) \tag{3.10}$$

Thus, model parameter surface is found below;

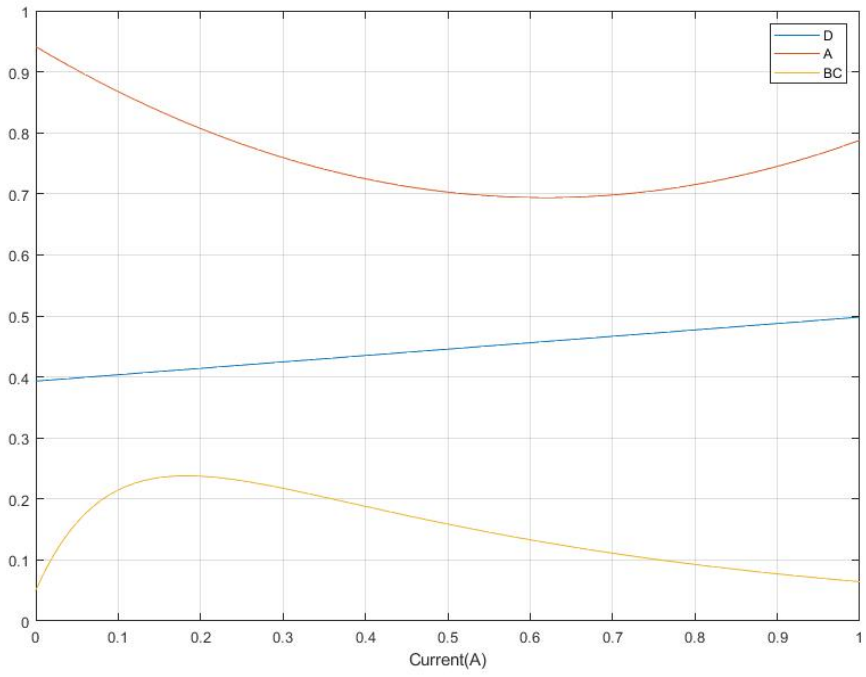

Figure 3.9 : Fitted Function for Model Parameters.

Now, the LPV model is obtained. To validate that model, test data is used. Results are shown below;

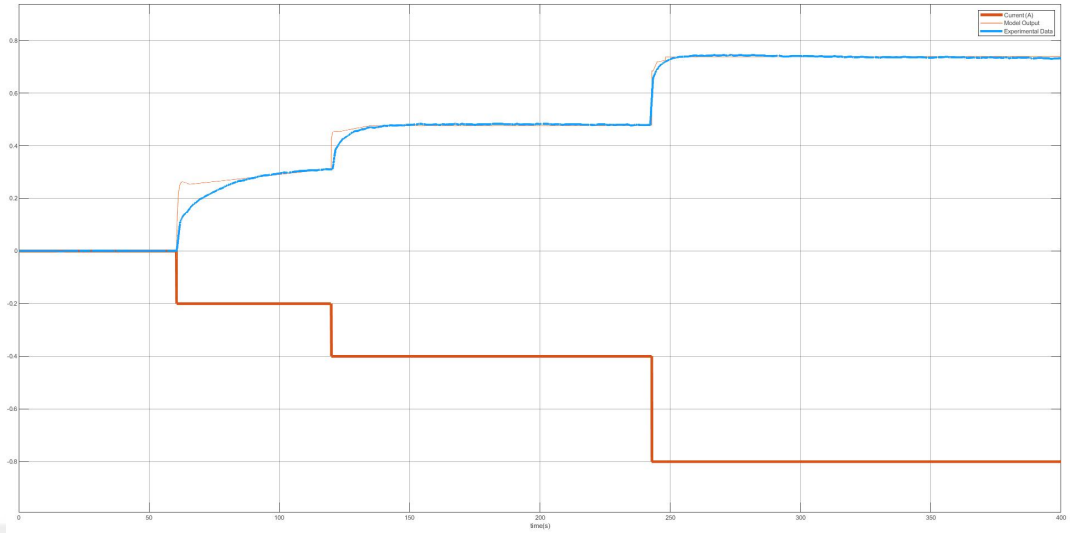

Figure 3.10 : Model Output Over Test Data.

Results show that obtained & validated model is capable to represent battery potential loss accurately. To reach a complete cell model, SOC-OCV curve implementation needs to be added.

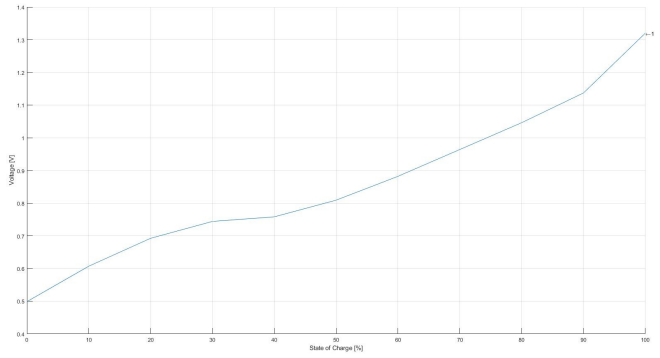

Figure 3.11 : Voltage Derivation against State of Charge.

Consequently, that curve is implemented and a complete battery cell is developed.

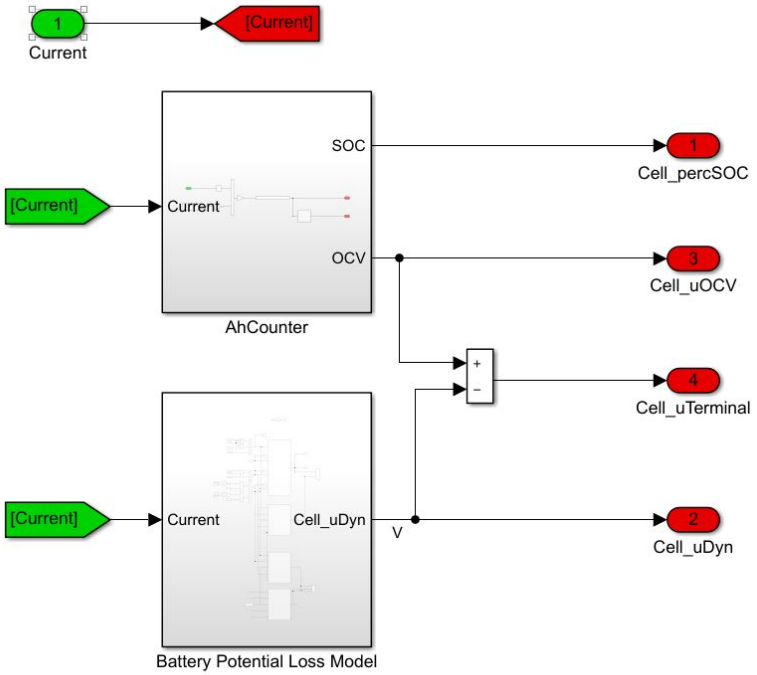

Figure 3.12 : Implemented Battery Model.

4. STATE OF CHARGE ESTIMATION

As mentioned, the state of charge is not directly measurable but it is an important parameter. Having an accurate and reliable state of charge parameter helps efficiently handling of the battery and ensures safety.

In the literature, there are several methods are proposed. Each method has some advantages and disadvantages. For that work, the coulomb counting method will be compared with the extended Kalman filter method. These methods are explained in this chapter.

4.1 Coulomb Counting Method

This method is also known as the ampere-hour counter. It is widely used in the industry because of its simplicity. That method focuses the output of the current sensor that measures during the battery's charge or discharge current and integrates to derive the state of charge.

$$SOC(t) = SOC(t-1) + \frac{I(t)}{Q}\delta t \tag{4.1}$$

The implementation of the Coulomb counting method is straightforward and memory efficient, but it has drawbacks.

- Noisy current measurements could have big impacts due to the integrator in the formula.
- Error drift due to the previously incorrectly estimated values.
- Current loses inside the battery and auxiliaries also taken into account into the formula.
- Battery degradation and temperature changes could influence the precision of the method

By using re-calibration points and providing reliable current measurement, that method could provide an accurate state of charge values.

The implementation as follows:

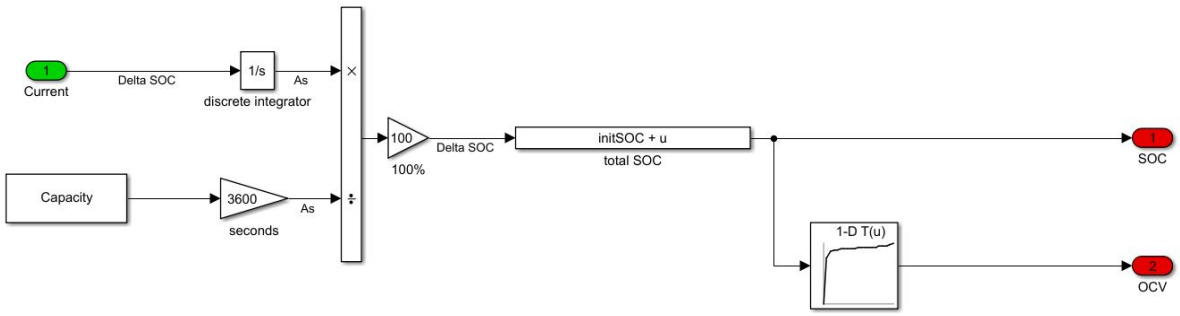

Figure 4.1 : Coloumb Counting Implementation.

4.2 Extended Kalman Filter Method

The Kalman filter is an estimation theory for estimating the immeasurable states of the system. The filter uses linear optimal filtering to give a recursive solution for predicting system state variables. If the system is nonlinear, at each step a linearization procedure is used to approximate the nonlinear system by linear time-varying system. [23] Using this linear time-varying system in Kalman Filter results in an extended Kalman filter for a nonlinear system.

In this case, the state of charge parameter is estimated by using current and voltage measurements. The estimated cell voltage is going to be compared to the actual measured voltage, then the obtained error term is also considered inside the state of charge estimation algorithm.

The extended Kalman filter algorithm consists of two main steps:

- State Prediction Step
- Measurement Correction Step

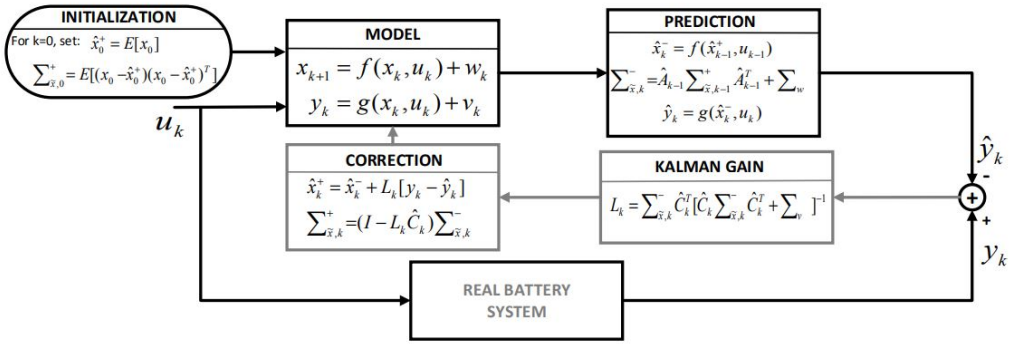

Figure 4.2 : Procedure of Extended Kalman Filter Algorithm [12].

The implementation procedure starts with finding state space model equations of the system, then the EKF procedure can be constructed as explained in Figure 4.2.

4.2.1 Implementation

The model that proposed in previous chapter as shown below:

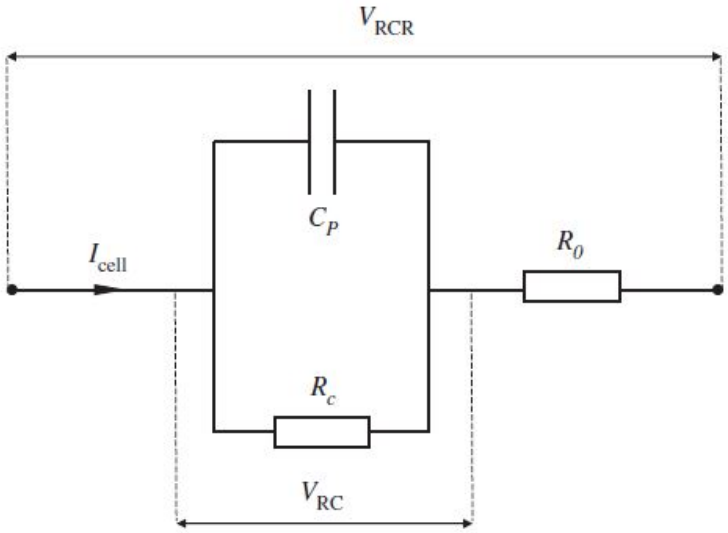

Figure 4.3 : First Order Thevenin equivalent battery model.

System equations could be written as follows:

$$V_{RC}(k+1) = (1 - \frac{\tau_s}{R_c C_p}) V_{RC}(k) + \frac{\tau_s}{C_p} I_{Cell}(k) \quad \textbf{(4.2)}$$

$$V_{RCR}(k) = V_{RC}(k) + R_0 I_{Cell}(k) \quad \textbf{(4.3)}$$

Now, equations will be written to have a state space model of the system.

$$SOC(t) = SOC(t-1) + \frac{\delta t}{Q} I(t) \tag{4.4}$$

$$\frac{dV_{RC}}{dt} = \frac{I_{Cell}}{C_p} - \frac{V_{RC}}{R_c C_p} \tag{4.5}$$

As a result, the following state equation is obtained for the battery model.

$$\frac{d}{dt}\begin{bmatrix} SOC(k+1) \\ V_{RC}(k+1) \end{bmatrix} = \begin{bmatrix} 0 & 0 \\ 0 & \frac{-1}{R_c C_p} \end{bmatrix} \begin{bmatrix} SOC \\ V_{RC} \end{bmatrix} + \begin{bmatrix} \frac{\delta t}{Q} \\ \frac{1}{C_p} \end{bmatrix} I_{cell} \tag{4.6}$$

$$V_{RCR} = f(OCV, SOC) - R_0 I_{cell} - V_{RC} \tag{4.7}$$

The equations of extended Kalman filter written as following:

$$x_{k+1} = f(x_k, u_k) + w_k \tag{4.8}$$

$$y_k = g(x_k, u_k) + v_k \tag{4.9}$$

w_k is zero mean Gaussian white noise that represents the non-measurable process noise that affects the system response, u_k is Gaussian white noise with a mean of zero that represents the sensor measurements and affects the system output and it has no memory effect on the system state.

At each time step, f and g functions are linearized around the operation point by using the Taylor series approximation. Thus, A, B, C, and D functions are expressed as follows:

$$A_k = \frac{\partial f(x_k, u_k)}{\partial x_k} = \begin{bmatrix} 1 & 0 \\ 0 & 1 - \frac{\delta t}{R_c C_p} \end{bmatrix} \tag{4.10}$$

$$B_k = \frac{\partial f(x_k, u_k)}{\partial u_k} = \begin{bmatrix} -\frac{\delta t}{Q} \\ \frac{1}{C_p} \end{bmatrix} \tag{4.11}$$

$$C_k = \frac{\partial g(x_k, u_k)}{\partial x_k} = \begin{bmatrix} 1 & -1 \end{bmatrix} \tag{4.12}$$

$$D_k = \frac{\partial g(x_k, u_k)}{\partial u_k} = \begin{bmatrix} -R_0 \end{bmatrix} \tag{4.13}$$

Hence, the specified equations are implemented in MATLAB-Simulink.

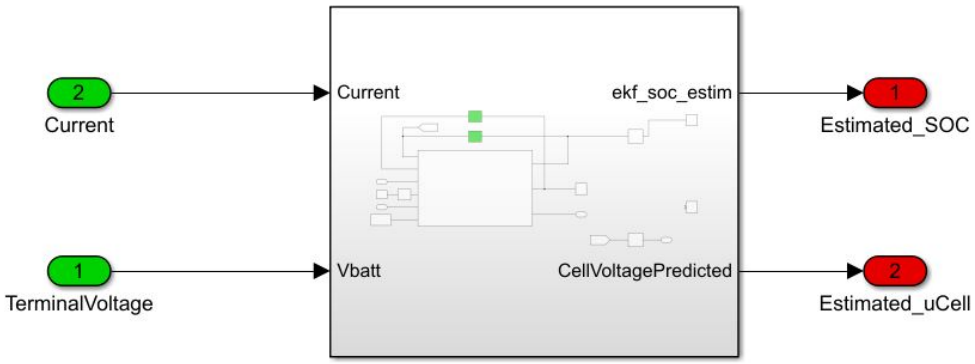

Figure 4.4 : Extended Kalman Filter Block.

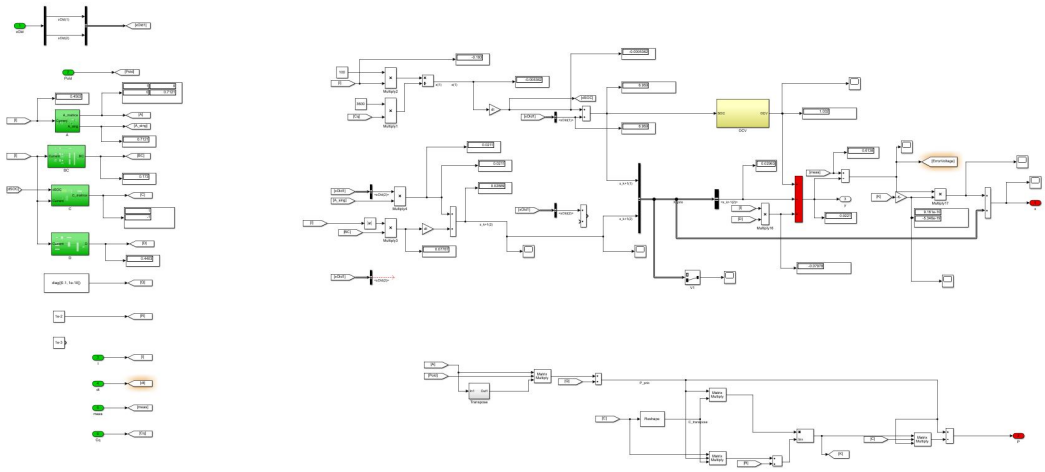

Figure 4.5 : Extended Kalman Filter Implementation in Simulink.

4.3 Simulation Results

It is known that in the simulation environment, the coulomb counting method works perfectly since there it is ideal conditions. Hence, obtained EKF model can be validated by comparing the coulomb counting method.

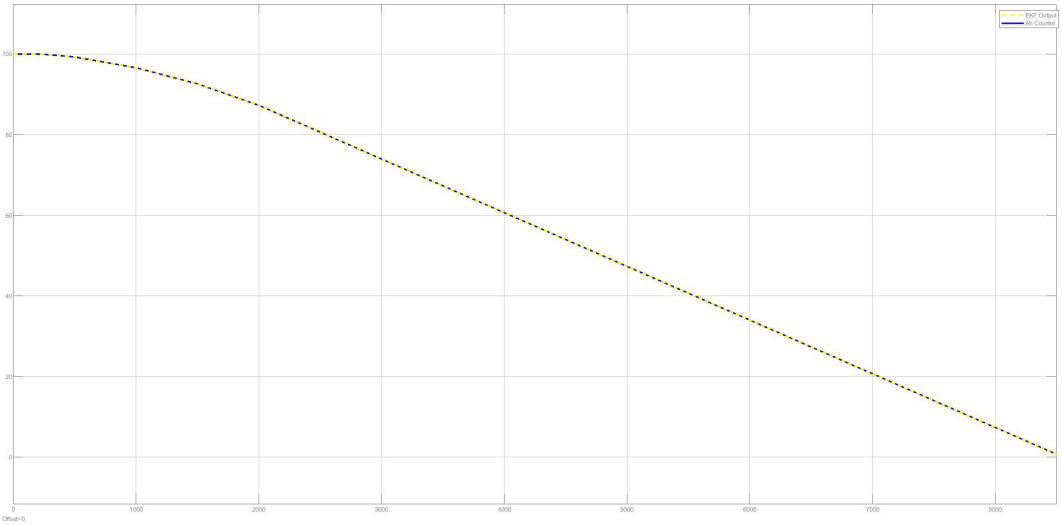

Figure 4.6 : EKF model validation against Coulomb Counter Method.

Now, confidence in our EKF model is gained.

To be able to simulate real life scenarios as much as possible, noisy measurement data is applied to the system to see the state of charge estimation behaviour of EKF. As it can be seen in Figure 4.7 and Figure 4.8, the applied extended Kalman filter precisely estimates the state of charge value.

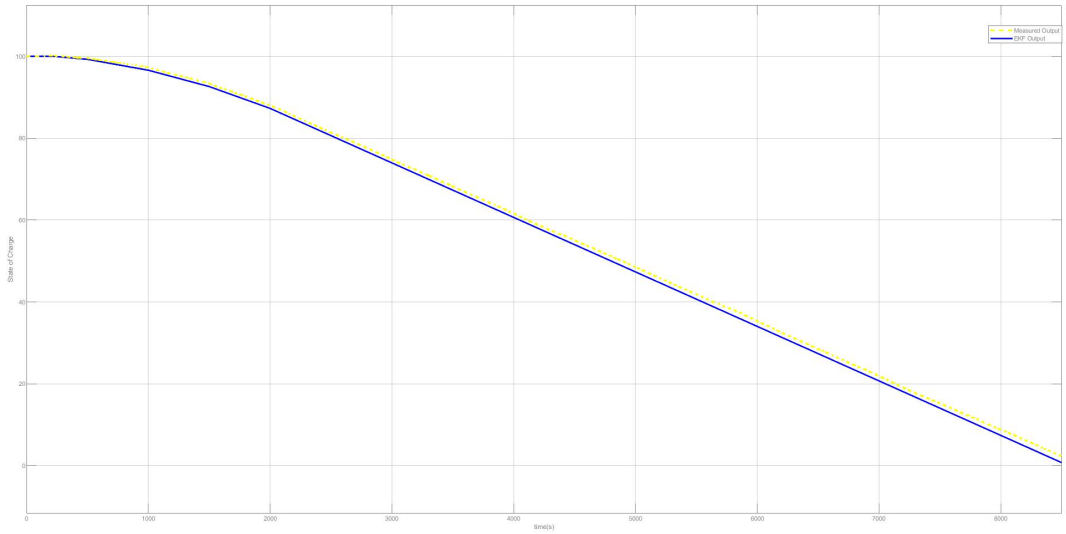

Figure 4.7 : EKF SoC estimation against measurement data.

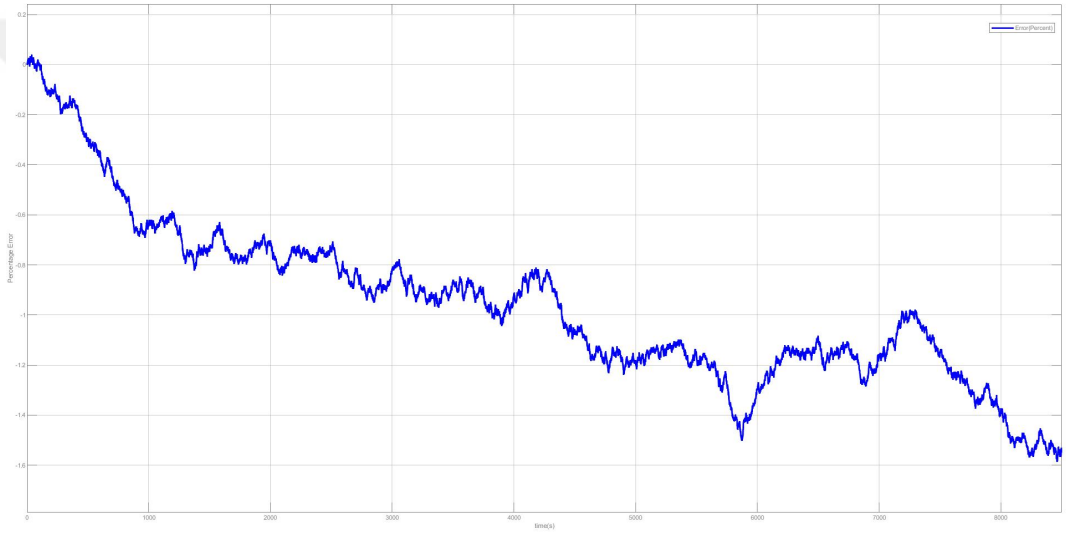

Figure 4.8 : EKF Obtained SoC Error Signal.

Due to the nonlinear nature of the model, small voltage and current deviations or measurement noise could create a big difference in the state of charge estimation.

But, with the help of the extended Kalman filter approach, noisy data could be filtered and state of charge estimation can be done precisely with less than 2 percent value.

5. CONCLUSIONS AND RECOMMENDATIONS

The purpose of the thesis is to provide an accurate state of charge estimation for zinc-air batteries.

First, cell modeling by using equivalent circuit modeling methods is studied. Then, an LPV model was developed for zinc-air type battery from different linear models to predict the nonlinear dynamic behaviour of the battery. After validating the model against test data, results showed that identified LPV model is able to represent the dynamic behaviour of the battery.

Thus, the battery model is used to estimate the state of charge estimation by using the ampere-hour counter method. After that, Extended Kalman Filter is applied to the developed model and compared to the real data. Even though the nature of the battery chemistry is not stable and having only an in-house battery data set, it is shown that the state of charge could be estimated accurately.

5.1 Recommendations for Future Work

As future work, the training data could be improved by using standardized load profiles(HPPC, NEDC, WLTP), testing against temperature changes, adding aging parameters. Also by only using available test data, charge behaviour could only be partially modelled. With the future improvements in the zinc-air battery chemistry in the literature, charging behaviour could also be modelled more in detail.

The study is also open for further improvements such as creating battery packs that represent real electric vehicles that could also give hints about the usability of the zinc-air batteries in real vehicles and systems.

Also for future reference, the battery industry will expand in favour of metal-air battery chemistry, and those chemistries are going to be employed in almost all secondary battery applications.

REFERENCES

[1] **Zhang, X.**, **Wang, X.G.**, **Xie, Z. and Zhou, Z.** (2016). Recent progress in rechargeable alkali metal–air batteries, *Green Energy Environment*, *1*(1), 4–17, https://www.sciencedirect.com/science/article/pii/S246802571630019X.

[2] **Lao-atiman, Arpornwichanop, A. and Kheawhom, S.** (2019). Discharge performance and dynamic behavior of refuellable zinc-air battery, *Scientific Data*, *6*(168).

[3] Lead Acid Batteries, https://sinovoltaics.com/learning-center/storage/lead-acid-batteries/, accessed: 2021-10-20.

[4] **Johnson, S.C.**, **Todd Davidson, F.**, **Rhodes, J.D.**, **Coleman, J.L.**, **Bragg-Sitton, S.M.**, **Dufek, E.J. and Webber, M.E.**, (2019). Chapter Five - Selecting Favorable Energy Storage Technologies for Nuclear Power, **H. Bindra and S. Revankar**, editors, Storage and Hybridization of Nuclear Energy, Academic Press, pp.119–175, https://www.sciencedirect.com/science/article/pii/B9780128139752000053.

[5] **Fetcenko, M.**, **Koch, J. and Zelinsky, M.**, (2015). 6 - Nickel–metal hydride and nickel–zinc batteries for hybrid electric vehicles and battery electric vehicles, **B. Scrosati**, **J. Garche and W. Tillmetz**, editors, Advances in Battery Technologies for Electric Vehicles, Woodhead Publishing Series in Energy, Woodhead Publishing, pp.103–126, https://www.sciencedirect.com/science/article/pii/B9781782423775000066.

[6] **Chawla, N.**, **Bharti, N. and Singh, S.** (2019). Recent Advances in Non-Flammable Electrolytes for Safer Lithium-Ion Batteries, *Batteries*, *5*.

[7] LFP battery, https://sinovoltaics.com/energy-storage/batteries/lfp-battery/, accessed: 2021-10-20.

[8] **Wang, C.**, **Yu, Y.**, **Niu, J.**, **Liu, Y.**, **Bridges, D.**, **Liu, X.**, **Pooran, J.**, **Zhang, Y. and Hu, A.** (2019). Recent Progress of Metal–Air Batteries—A Mini Review, *Applied Sciences*, *9*(14), https://www.mdpi.com/2076-3417/9/14/2787.

[9] **Olaru, S.**, **Golovkina, A.**, **Lao-atiman, W. and Kheawhom, S.** (2019). A Mathematical Model for Dynamic Operation of Zinc-Air Battery Cells, *IFAC-PapersOnLine*, *52*(17), 66–71,

https://www.sciencedirect.com/science/article/pii/S2405896319309632, 7th IFAC Symposium on System Structure and Control SSSC 2019.

[10] **Gu, P.**, **Zheng, M.**, **Zhao, Q.**, **Xiao, X.**, **Xue, H. and Pang, H.** (2017). Rechargeable zinc–air batteries: a promising way to green energy, *J. Mater. Chem. A*, *5*, 7651–7666, http://dx.doi.org/10.1039/C7TA01693J.

[11] **Lao-atiman, W.**, **Olaru, S.**, **Diop, S.**, **Skogestad, S.**, **Arpornwichanop, A.**, **Cheacharoen, R. and Kheawhom, S.** (2020). Linear parameter-varying model for a refuellable zinc-air battery, *Royal Society Open Science*, *7*(12), 201107.

[12] **Rivera-Barrera, J.P.**, **Muñoz-Galeano, N. and Sarmiento-Maldonado, H.O.** (2017). SoC Estimation for Lithium-ion Batteries: Review and Future Challenges, *Electronics*, *6*(4), https://www.mdpi.com/2079-9292/6/4/102.

[13] **IEA** (2021). Global EV Outlook 2021, **Technical Report**, International Energy Agency, Paris.

[14] **Beelen, H.** (2019). Model-based temperature and state-of-charge estimation for Li-ion batteries, *Ph.D. Dissertation*, Electrical Engineering, proefschrift.

[15] **Scrosati, B. and Garche, J.** (2010). Lithium batteries: Status, prospects and future, *Journal of Power Sources*, *195*(9), 2419–2430.

[16] **Committee, B.T.**, (2021). Battery Terminology, https://0-doi-org.divit.library.itu.edu.tr/10.4271/J1715/2_202108.

[17] Battery Energy Storage White Paper, http://www.suschem.org/files/library/Suschem_energy_storage_final_preview.pdf, accessed: 2021-10-20.

[18] **Thackeray, M.**, **David, W.**, **Bruce, P. and Goodenough, J.** (1983). Lithium insertion into manganese spinels, *Materials Research Bulletin*, *18*(4), 461–472, https://www.sciencedirect.com/science/article/pii/0025540883901381.

[19] **Zhang, J.**, **Zhou, Q.**, **Tang, Y.**, **Zhang, L. and Li, Y.** (2019). Zinc–air batteries: are they ready for prime time?, *Chem. Sci.*, *10*, 8924–8929, http://dx.doi.org/10.1039/C9SC04221K.

[20] **Zhang, X.**, **Wang, X.G.**, **Xie, Z. and Zhou, Z.** (2018). Translating Materials-Level Performance into Device-Relevant Metrics for Zinc-Based Batteries, *Joule*, *2*(12), 2519–2527.

[21] **Zhang, C.**, **Allafi, W.**, **Dinh, Q.**, **Ascencio, P. and Marco, J.** (2018). Online estimation of battery equivalent circuit model parameters and state of charge using decoupled least squares technique, *Energy*, *142*, 678–688, https://www.sciencedirect.com/science/article/pii/S0360544217317127.

[22] **He, H.**, **Xiong, R. and Fan, J.** (2011). Evaluation of Lithium-Ion Battery Equivalent Circuit Models for State of Charge Estimation by an Experimental Approach, *Energies*, *4*(4), 582–598, https://www.mdpi.com/1996-1073/4/4/582.

[23] (2014). A novel on-board state-of-charge estimation method for aged Li-ion batteries based on model adaptive extended Kalman filter, *Journal of Power Sources*, *245*, 337–344, https://www.sciencedirect.com/science/article/pii/S0378775313011154.

CURRICULUM VITAE

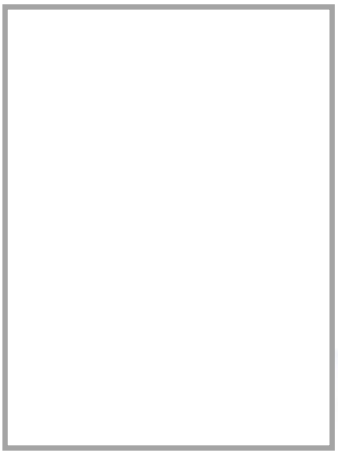

Name Surname : Burak SATILMIŞOĞLU

EDUCATION :

- **MSc.** : 2021, Istanbul Technical University, Graduate School Of Science, Department of Control and Automation Engineering
- **BSc.** : 2017, Istanbul Technical University, Faculty of Electrical and Electronics Engineering, Department of Control and Automation Engineering

PROFESSIONAL EXPERIENCE AND REWARDS:

- (2021 - ...) DAF Trucks N.V. - Embedded Software Engineer
- (2017-2021) FEV Türkiye - Electric Vehicle Systems Engineer